Temperature-Dependent Electrical Characterization of a Thermally Sensitive Hepatic Tumor Phantom

Ahmet Bilir*, Sema Dumanli†,
*Electrical and Electronics Engineering, Bogazici University, Istanbul, Turkey, ahmet.bilir, sema.dumanli@boun.edu.tr

***Abstract*—Phantom design is a critical task in biomedical device development which gives a strong indication of validity before going for animal/human testing. Microwave ablation therapy is no exception. The temperature change in the target tissue is measured in thermal phantoms after being estimated with electromagnetic and thermal simulations. Establishing a visual feedback mechanism during thermal therapy would bring the testing process closer to more real-time testing. Here we propose a semi-transparent polyacrylamide gel-based hepatic tumor phantom at 2.45 GHz of which absorbance changes as the temperature increases. It is shown that the phantom can be optimized such that the absorbance converges to its maximum value at a specific target temperature value. The temperature-dependent permittivity and conductivity values and temperature-dependent absorbance values of the proposed phantom are given.**

***Index Terms*—thermally sensitive phantom, polyacrylamide gel based phantom, microwave ablation**

I. Introduction

Thermal ablation is an established method to eradicate cancerous cells. Since the cause of the damage in the target tissue is a temperature rise, it should be carefully monitored so that the damage is kept inside the cancerous region. To achieve this, temperature maps are created to map the temperature change for a given output power for accurate ablation planning [1]. Maps can be created using various methods including numerical and experimental approaches. The experimental mapping using thermal phantoms is a crucial step before moving on to animal/human testing. Ex-vivo tissues can be utilized as thermal phantoms for experimental mapping [2] however the properties of the tissue change drastically post-mortem. Therefore, scientists have been focusing on developing gel phantoms mimicking the electrical and thermal properties of the target tissues [1].

Various types of phantom recipes have been proposed in the literature such as gellan gum based phantoms [3], hydroxyethyl cellulose (HEC) based phantoms [4], gelatin based phantoms [5], bovine serum albumin (BSA) based phantoms [6], and polyacrylamide gel (PAG) based phantoms [7]. Among these recipes, the ones that are suitable for microwave ablation are of interest for this study [6][4][7]. Note that, microwave ablation offers several benefits including increased temperature, a larger area of tissue removal, and reduced treatment duration as compared to other thermal therapies. In [7], a transparent thermal phantom operating at 2.45 GHz was proposed. Getting visual feedback during the test phase would greatly simplify the mapping hence a transparent phantom is a good starting point. However, the phantom proposed in [7] is not temperature sensitive, i.e. temperature change does not change its optical properties which would result in visual feedback for the observer.

In the literature, phantoms visually responding to temperature have been proposed [8][9][10]. [8] proposes a carrageenan gel based phantom which mimics the electrical properties of muscle at 900 MHz and 1.45 GHz. As the temperature rises from $35°$C to $47°$C , the color of the phantom changes from red to blue. Similarly, [9] and [10] propose thermochromic pigments loaded PAG based tissue phantoms of which color changes with temperature. Note that neither electrical properties of the phantoms, nor the target tissue were provided for these studies. A different approach was taken in [11] where the phantom turns opaque as the temperature rises and it is based on N-isopropylacrylamide (NIPAM). The electrical properties however are missing in this recipe as well. Changing the opacity of the phantom as the temperature changes, [12] and [13] mixed PAG and BSA. This approach is aligned with the aim of this study where visual feedback can be obtained as the target tissue is heated. Both studies lack electrical properties analysis at microwave region. Tuning the thermal and electrical properties of this family of phantoms simultaneously is challenging as modifications to key ingredients aimed at tuning one property invariably exert an influence on the other. Here, a PAG and BSA based hepatic tumor phantom is developed to operate at 2.45 GHz. Two sets of recipes are provided where thermal properties are tuned to turn opaque at $45°$C and $60°$C to get visual feedback for microwave hyperthermia and ablation respectively. This phantom is going to be used to validate the simultaneous microwave ablation and monitoring system proposed in [14] by the authors.

Section II, the phantom recipe is detailed where the effects of glycerin, acrylamide, BSA, salts, and initiator-activator are discussed, each addressing their respective impacts. Section III presents the analysis of optical and electrical properties against temperature. The paper concludes in Section IV.

II. Phantom Development

The temperature-sensitive phantom development procedure is adapted from the method described in [13]. The phantom is based on polyacrylamide gel to mimic the elastic properties of soft tissues [12]. Acrylamide and N, N methylene-bis-acrylamide (bis) dissolved in water solidifies by a polymerization reaction initiated by the initiator-activator pair; L-ascorbic acid, $FeSO_4$, and H_2O_2. As a temperature-sensitive indicator,

lyophilized powder bovine serum albumin (BSA) is used. The temperature level that BSA coagulates is adjusted by the chemical buffer consisting of the salts citric acid monohydrous (CAM) and sodium citrate dehydrate (SCD). The details about the chemical buffer and polymerization of acrylamide-bis can be found in [12]. Finally, glycerin is utilized the reduce the dielectric constant of the water.

TABLE I
TEMPERATURE SENSITIVE PHANTOM RECIPE MIMICKING THE ELECTRICAL PROPERTIES OF THE HEPATIC TUMOR AT 2.45 GHZ WHERE THE ABSORBANCE CONVERGENCE VALUE IS 60°C.

Solution	Quantity
Glycerin	810 μL
Acrylamide-bis	660 μL
CAM - SCD	330 μL
BSA	600 μL

Solution	Quantity
L-ascorbic acid	30 μL
$FeSO_4$	30 μL
H_2O_2	6 μL

For each ingredient mentioned in the previous paragraph, a stock solution is prepared to facilitate the phantom preparation. At first, 10 mL glycerin and 10 mL deionized water are mixed in a 50 mL falcon tube until the solution is homogeneous. Then, 6 gr of acrylamide and 0.15 gr of N, N methylene-bis-acrylamide is dissolved in 10 mL of deionized water. After the ingredients are dissolved, deionized water is added to the solution until the volume of the solution is 20 mL. Similarly, 1 gr of citric acid monohydrous and 1 gr of sodium citrate dehydrate are dissolved in 10 mL of water, and water is added to obtain 20 mL of the solution. Then, 2 gr of BSA is dissolved in 10 mL of water. For the initiator-activator pair, 1 gr of L-ascorbic acid is dissolved in 10 mL of water, 0.1 M $FeSO_4$ solution is diluted by a ratio of 1:10, and 50% H_2O_2 is used. The recipe for the temperature-sensitive phantom which mimics the electrical properties of the hepatic tumor at 2.45 GHz is given in Table I. The total volume of the phantom given in the recipe is 2466 μL, which is prepared in the cuvettes to measure the optical properties of the phantom using a spectrophotometer. The ingredients except for the initiator-activator pair given in the recipe are mixed gently in a 15 mL falcon tube until the mixture is homogeneous. Lastly, the initiator-activator pair is added, mixed, and poured into the cuvettes. The polymerization takes approximately ten minutes. Note that the polymerization is an exothermic reaction and it may cause precoagulation of the BSA. Therefore, before the initiator-activator pair is added, the solution is stored in a refrigerator until its temperature is about $4-8$°C. Note that, the coagulation of BSA is irreversible. Fig. 1 shows the freshly prepared transparent and completely coagulated phantom samples in the cuvettes.

The electrical conductivity of the phantom is affected mainly by glycerin and CAM-SCD solutions but CAM-SCD solution determines the coagulation temperature of the BSA and the permittivity of the solution is controlled by the amount of glycerin. Therefore, the amounts of these ingredients should

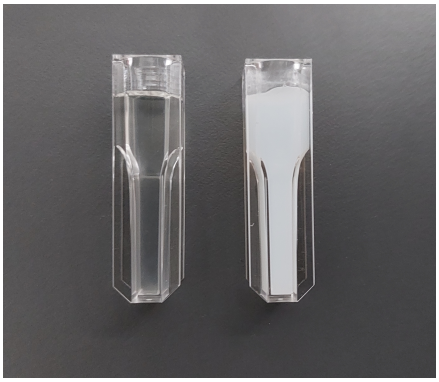

Fig. 1. The phantom in the cuvettes (a) at room temperature and (b) exposed to 80°C water for one minute.

be meticulously adjusted to achieve the correct permittivity, conductivity, and coagulation temperature.

The following subsections discuss the effect of each ingredient on the electrical properties and the the temperature-dependent electrical and optical properties are provided in Section III.

A. The Effect of Glycerin

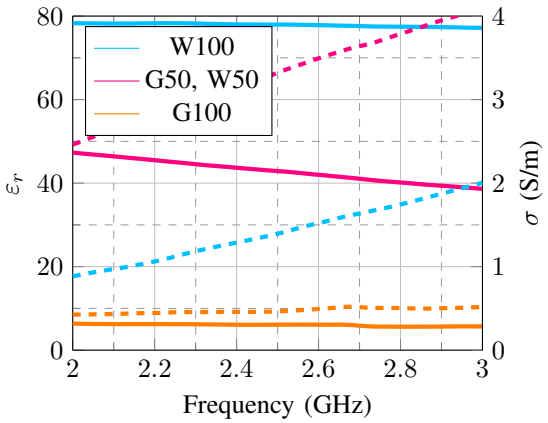

Fig. 2. The electrical properties of different glycerin-water solutions. Solid and dashed lines represent ε_r and σ, respectively.

Fig. 2 shows the electrical properties of the water, glycerin, and glycerin-water solution. W100, G50-W50, and G100 represent the percentage volume of the solutions. The electrical properties are measured by an open-ended coaxial probe, SPEAG DAK 3.5. Glycerin's permittivity and conductivity are 6.5 and 0.5 S/m at 2.45 GHz, which are low compared to water. When it is dissolved in water, the conductivity increases to a value, 3.5 S/m, greater than the conductivity of water whereas the permittivity drops to 43. Hence, the dielectric constant of the solution can be adjusted by adding a certain amount of glycerin to water.

B. The Effect of Acrylamide

Fig. 3 shows the effect of the acrylamide on the electrical properties before and after the polymerization. The percentage

amount of acrylamide and N, N methylene-bis-acrylamide are the same as the phantom recipe but in order to observe the effect on the electrical properties, other ingredients are not included. The permittivity of the liquid form is less than water whereas it increases the conductivity. After the polymerization, the dielectric constant drops further, and conductivity decreases, too. Note that the greater amount of acrylamide results in a greater increase in the temperature during the polymerization, therefore the greater amount of acrylamide may cause pre-coagulation of BSA.

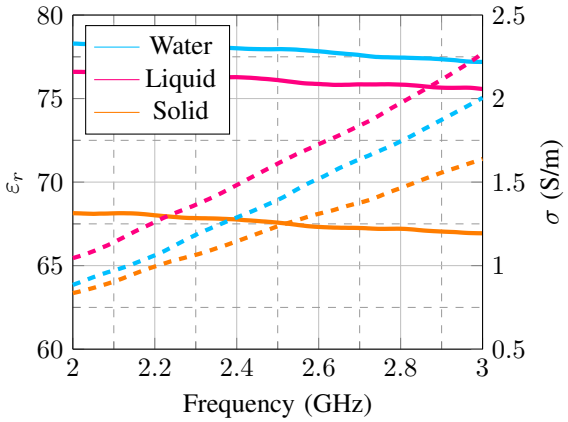

Fig. 3. The effect of the polymerization of the acrylamide-bis solution on the electrical properties. Solid and dashed lines represent ε_r and σ, respectively.

C. The Effect of Bovine Serum Albumin

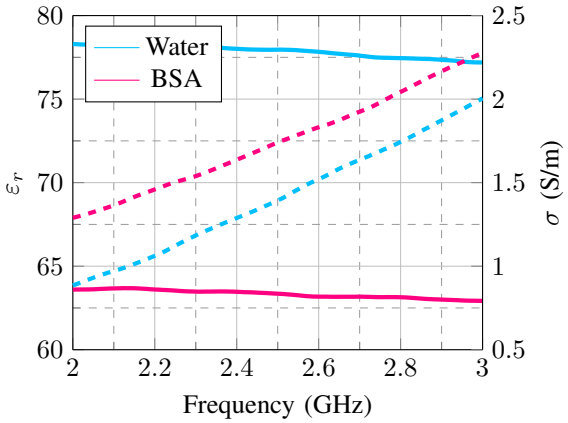

Fig. 4. The effect of the BSA solution on the electrical properties. Solid and dashed lines represent ε_r and σ, respectively.

Fig. 4 shows the effect of the lyophilized powder bovine serum albumin (BSA) on the electrical properties. 2 gr of BSA is dissolved in 10 mL of water. Note that the mixture is stirred gently in order to prevent frothing. The addition of BSA in water has a more limited effect on the dielectric constant and conductivity compared to other ingredients. It reduces the permittivity to 63 and increases the conductivity to 1.75 S/m at 2.45 GHz. Although it may be utilized to decrease the permittivity, in order to reduce the cost of the phantom, glycerin is preferred.

D. The Effect of Salts

Fig. 5 shows the effect of the chemical buffer consisting of the citric acid monohydrous and sodium citrate dehydrate on the electrical properties. The percentage amounts of the salts are the same as the phantom recipe but in order to observe its effect on the electrical properties, other phantom ingredients are not included. The salts increase the conductivity of the water to 1.6 S/m and decrease the relative permittivity to 75. Note that the salts are used to lower the pH of the solution, hence it determines the coagulation temperature of the BSA. This results in a dependency between the coagulation temperature and conductivity. Hence, the amount of the salts and glycerin should be adjusted carefully.

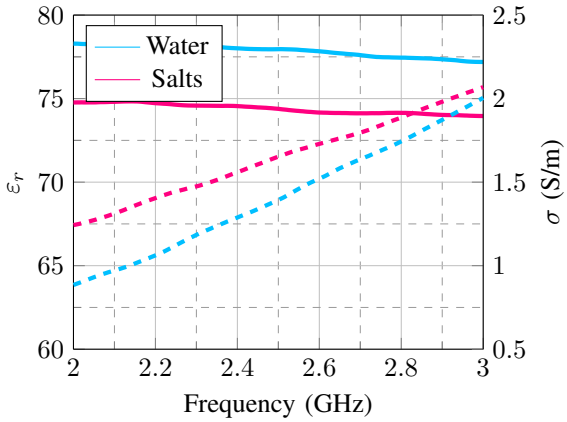

Fig. 5. The effect of the chemical buffer on the electrical properties. Solid and dashed lines represent ε_r and σ, respectively.

E. The Effect of Initiator-Activator Pair

Since the amount of initiaor-activator pair is quite low compared to the phantom volume, it has a minimal effect on the electrical properties of the phantom, hence it can be neglected.

III. Measurements and Results

The temperature-dependent optical and electrical properties of the developed phantoms are measured using an incubator (Nukleon NCI-55), two thermometers, a spectrophotometer (Persee T6 UV/ VIS 190 - 1100 nm), and a dielectric assessment kit (SPEAG DAK 3.5). Each prepared phantom is set in a pair of containers to have a main sample and a shadow sample. One thermometer is used to track the precise temperature near the main sample in the incubator. The second thermometer is located inside the shadow sample which is located next to the main sample. By doing so, we are keeping track of the precise temperature inside the main sample without locating a probe in it. The incubator temperature is set to the target value, and as the thermal equilibrium is reached in both thermometers, both samples are taken out. They are located

inside the spectrophotometer for optical analysis or under the dielectric probe for electrical analysis. As the measurements are taken, the temperature of the shadow sample is tracked to make sure the temperature is kept within a certain deviation during the measurement. The data presented here are taken under 3°C deviation. Note that each measurement is repeated three times. The optical set-up can be seen in Fig. 6.

Fig. 6. The measurement setup to determine the temperature-dependent optical properties of the phantom.

A. Optical Properties

The temperature-dependent optical properties are measured using the set-up previously described in Section III. Fig. 7 presents how the absorbance changes as the temperature increases at various wavelength values at the visible light spectrum. The visual feedback mechanism can be observed where the absorbance converges at 60°C. This will allow the ablated region to be visible to an observer as microwave ablation is conducted.

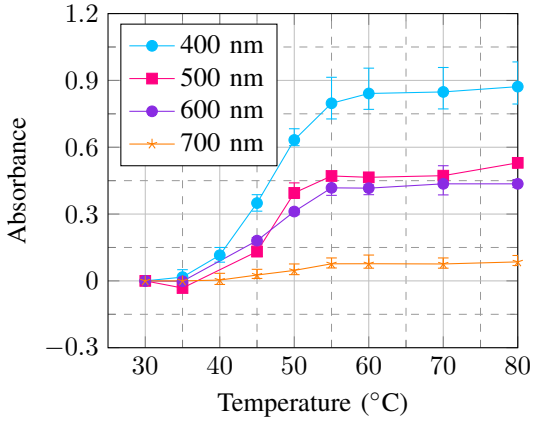

Fig. 7. The measured temperature dependent absorbance values for the developed phantom at various wavelength values at the visible spectrum.

Note that the visual feedback mechanism can be tuned such that the absorbance converges at a different temperature. If this phantom was used to visually observe microwave hyperthermia which occurs at 45°C, then the amount of salts should be increased to lower the pH of the solution so that the coagulation temperature of the BSA is reduced as listed in Table II. Fig. 8 shows the temperature-dependent optical values of re-tuned phantom along with the phantom developed to converge at 60°C.

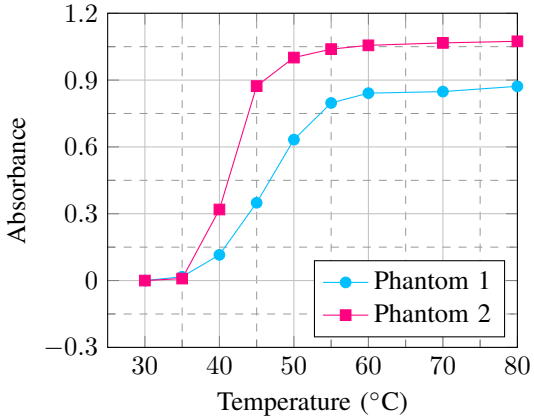

Fig. 8. The measured temperature dependent absorbance values for two phantoms developed to convergence at two temperature values: 45°C (microwave hyperthermia) and 60°C (ablation).

TABLE II
THE RECIPES FOR TWO DIFFERENT PHANTOMS SENSITIVE TO TWO DIFFERENT TEMPERATURE VALUES.

Solution	Phantom 1	Phantom 2
Glycerin	810 μL	750 μL
Acrylamide-bis	660 μL	600 μL
CAM - SCD	330 μL	450 μL
Bovine serum albumin	600 μL	600 μL
L-ascorbic acid	30 μL	30 μL
$FeSO_4$	30 μL	30 μL
H_2O_2	6 μL	6 μL

B. Electrical Properties

The temperature-dependent electrical properties are measured using the setup described previously. The dielectric constants of the phantom and the hepatic tumor given in the literature at 2.45 GHz at 37°C [15] are 55 and 52.8, respectively and conductivity comparison of the phantom and hepatic tumor are 1.95 S/m and 1.97 S/m, respectively. The dielectric constant and conductivity of the phantom deviate from the values given in the literature by 4.17% and 1.01%, respectively. Fig. 9 shows the temperature-dependent electrical properties of the phantom. The relative permittivity and conductivity decrease as the temperature increases. The comparison of the temperature-dependent electrical properties of the phantom and the hepatic tumor given in the literature at 2.45 GHz can be seen in Fig. 10 [15]. The reduction of the permittivity of the phantom is less than the values measured in the literature and the decrease in the conductivity of the phantom is greater. If the proposed phantom is used for ablation measurements, this discrepancy might result in an increase in ablation time. However, the trends are parallel to the literature. Note that the values in the literature are ex-vivo values hence this area begs for further investigation.

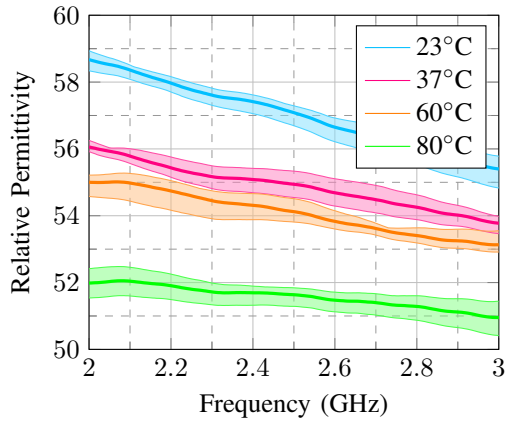

(a)

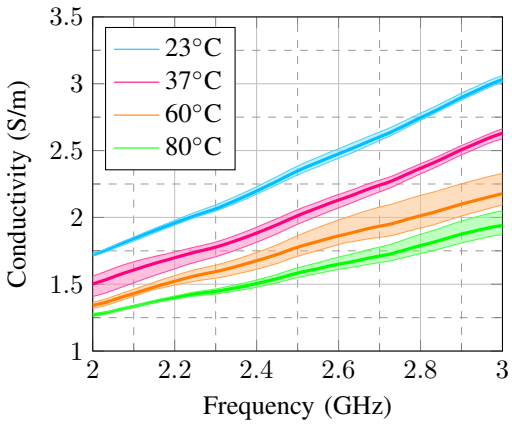

(b)

Fig. 9. Relative permittivity (a) and conductivity (S/m) (b) values vs frequency (GHz) measured as the phantom is heated up from room temperature to beyond ablation temperature (shaded areas represent the standard deviation as the measurements were repeated three times.

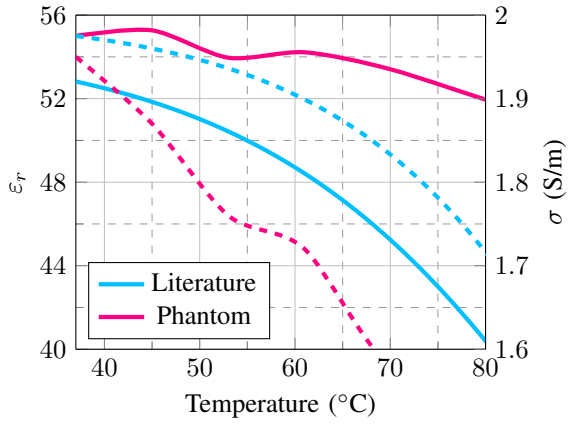

Fig. 10. The measured temperature dependent electrical properties of the developed phantom compared to the measured temperature dependent electrical properties of hepatic tumor at 2.45 GHz [15]. Solid and dashed lines represent ε_r and σ, respectively.

IV. Conclusion

In this paper, a recipe for a temperature-sensitive phantom mimicking the electrical properties of hepatic tumors at 2.45 GHz is presented. The phantom is transparent at room temperature and above a certain temperature threshold, which can be adjusted by the chemical buffer amount, opacifies. The optimized amounts for the ingredients for convergence at 45°C and 60°C are provided. By using this real-time visual feedback, initial microwave ablation and microwave hyperthermia tests can be conducted in a convenient way.

References

[1] M. S. Ahmad et al., 'Chemical Characteristics, Motivation and Strategies in choice of Materials used as Liver Phantom: A Literature Review', J Med Ultrasound, vol. 28, no. 1, pp. 7–16, Jan. 2020.

[2] Z. Ji and C. L. Brace, 'Expanded modeling of temperature-dependent dielectric properties for microwave thermal ablation', Phys Med Biol, vol. 56, no. 16, pp. 5249–5264, Aug. 2011, doi: 10.1088/0031-9155/56/16/011.

[3] R. K. Chen and A. J. Shih, 'Multi-modality gellan gum-based tissue-mimicking phantom with targeted mechanical, electrical, and thermal properties', Phys Med Biol, vol. 58, no. 16, pp. 5511–5525, Aug. 2013.

[4] P. Prakash, M. C. Converse, D. M. Mahvi, and J. G. Webster, 'Measurement of the specific heat capacity of liver phantom', Physiol Meas, vol. 27, no. 10, pp. N41-46, Oct. 2006.

[5] Y. Yuan et al., 'A heterogeneous human tissue mimicking phantom for RF heating and MRI thermal monitoring verification', Phys. Med. Biol., vol. 57, no. 7, p. 2021, Mar. 2012.

[6] I. Farhat, J. Farrugia, L. Farrugia, J. Bonello, D. Pollacco, and C. Sammut, 'The synthesis of a liver tissue mimicking solution for microwave medical applications', Biomed. Phys. Eng. Express, vol. 8, no. 6, p. 065014, Oct. 2022.

[7] A. Surowiec, P. N. Shrivastava, M. Astrahan, and Z. Petrovich, 'Utilization of a multilayer polyacrylamide phantom for evaluation of hyperthermia applicators', Int J Hyperthermia, vol. 8, no. 6, pp. 795–807, 1992.

[8] Y. Suzuki, M. Baba, M. Taki, K. Fukunaga, and S. Watanabe, 'Imaging the 3D temperature distributions caused by exposure of dielectric phantoms to high-frequency electromagnetic fields', IEEE Trans. on Dielectrics and Electrical Insulation, vol. 13, no. 4, pp. 744–750, Aug. 2006.

[9] A. H. Negussie et al., 'Thermochromic tissue-mimicking phantom for optimisation of thermal tumour ablation', Int J Hyperthermia, vol. 32, no. 3, pp. 239–243, May 2016.

[10] A. Dabbagh, B. J. J. Abdullah, N. H. Abu Kasim, and C. Ramasindarum, 'Reusable heat-sensitive phantom for precise estimation of thermal profile in hyperthermia application', Int J Hyperthermia, vol. 30, no. 1, pp. 66–74, Feb. 2014.

[11] J. Shieh et al., 'Acrylic acid controlled reusable temperature-sensitive hydrogel phantoms for thermal ablation therapy', Applied Thermal Engineering, vol. 62, no. 2, pp. 322–329, Jan. 2014.

[12] M. McDonald, S. Lochhead, R. Chopra, and M. J. Bronskill, 'Multi-modality tissue-mimicking phantom for thermal therapy', Phys Med Biol, vol. 49, no. 13, pp. 2767–2778, Jul. 2004.

[13] Z. Bu-Lin, H. Bing, K. Sheng-Li, Y. Huang, W. Rong, and L. Jia, 'A polyacrylamide gel phantom for radiofrequency ablation', Int J Hyperthermia, vol. 24, no. 7, pp. 568–576, Nov. 2008.

[14] A. Bilir, O. K. Erden and S. Dumanli, "Coaxial Slot Antenna Array Design for Microwave Ablation and Monitoring," 2022 3rd URSI AT-AP-RASC, Gran Canaria, Spain, 2022, pp. 1-4.

[15] B. Radjenović, M. Sabo, L. Šoltes, M. Prnova, P. Čičak, and M. Radmilović-Radjenović, 'On Efficacy of Microwave Ablation in the Thermal Treatment of an Early-Stage Hepatocellular Carcinoma', Cancers (Basel), vol. 13, no. 22, p. 5784, Nov. 2021.